

Deliverable D4.2: Geomechanical characteristics of low permeability sandstones in potential geothermal reservoirs

WP 4: Demonstration of combined hydraulic-thermal-chemical treatments in sandstones, carbonate rocks and granites

Lead Beneficiary	TNO – Jan ter Heege
Type	<input checked="" type="checkbox"/> R - report, document etc. <input type="checkbox"/> OTHER - software, technical diagram etc. <input type="checkbox"/> DEM - demonstrator, pilot etc. <input type="checkbox"/> E - ethics <input type="checkbox"/> DEC - website, patent filing etc.
Status	<input type="checkbox"/> Draft <input checked="" type="checkbox"/> WP manager accepted <input checked="" type="checkbox"/> Project coordinator accepted
Dissemination level	<input checked="" type="checkbox"/> PU - Public <input type="checkbox"/> CO - Confidential: only for members of the consortium
Contributors	<input type="checkbox"/> 1-GFZ <input type="checkbox"/> 5-GES <input type="checkbox"/> 9-GTL <input type="checkbox"/> 13-SNU <input checked="" type="checkbox"/> 17-UU <input type="checkbox"/> 2-ENB <input checked="" type="checkbox"/> 6-TNO <input type="checkbox"/> 10-UoS <input type="checkbox"/> 14-KIC <input type="checkbox"/> 3-ESG <input type="checkbox"/> 7-ETH <input type="checkbox"/> 11-TUD <input type="checkbox"/> 15-ECW <input type="checkbox"/> 4-UoG <input type="checkbox"/> 8-GTN <input type="checkbox"/> 12-NEX <input type="checkbox"/> 16-WES
Creation date	24.02.2020
Last change	25.02.2020
Version	1
Due date	29.02.2020
Submission date	28.02.2020

Abstract

Subcritical fracturing can contribute to stimulation of permeability in geothermal reservoirs as it is observed to lead to lower formation breakdown pressure and enlargement of fracture disturbed zone. It may contribute to more efficient, low risk stimulation of reservoir permeability by (1) reduced injection rates and volumes required for stimulation, (2) better optimized stimulation, and (3) progressively increasing permeability and flow rates during operation of geothermal doublets. This study aims to explore methods to determine the contribution of subcritical crack growth to permeability increase during operation of a geothermal doublet targeting a tight sandstone reservoir in the Netherlands. It includes (1) a short review of the theory underpinning subcritical crack growth, (2) an analysis of typical experimental data for subcritical fracture growth velocities in sandstones, and (3) an analysis of hydro-mechanical properties of the tight Triassic sandstone targeted by the Trias Westland project in the Netherlands, including both axial compression and fluid injection experiments. The hydro-mechanical properties of the Triassic sandstone targeted by the Trias Westland project suggest that the reservoir is too tight to be considered for geothermal energy. Flow rates will be negligible unless the low reservoir permeability is restricted to the near-well area or high permeability zones exist that can be connected to wells using stimulation treatments. Core samples from the reservoir provide a unique opportunity to further study the effect of stimulation, including the effect of subcritical crack growth on permeability and strength.

Acknowledgements

Part of this report is based on an internship project by Emilio Cecchetti on “Time-Dependent Fracturing in Rocks to Tackle Tight Geothermal Reservoirs in the Netherlands”, performed at TNO to obtain an M.Sc. degree at Utrecht University. Emilio Cecchetti and co-supervisors Brecht Wassing (TNO) and Fred Beekman (UU) are gratefully acknowledged for their work. Holger Cremer (TNO) is thanked for arranging the research task on “subcritical fracturing in tight sandstones” that accommodated this research.

Table of Content

Abstract	2
Table of Contents	3
1. Introduction	4
2. Short review of subcritical crack growth theory	6
3. Experimental data for subcritical crack growth in sandstones	8
4. Hydro-mechanical properties of the Triassic sandstone targeted by the Trias Westland project	9
5. Discussion and Conclusions	11
6. References	13
Imprint	15

1. Introduction

DESTRESS targets stimulation of Enhanced Geothermal Systems with minimal seismicity. The concept of “Soft Stimulation” has been advanced, which aims to stimulate the permeability of tight reservoirs, while preventing large seismic events (Zang et al. 2013; Hofmann et al. 2018). One of the soft stimulation concepts is cyclic pumping (“fatigue hydraulic fracturing”), which involves cyclic increase and decrease of fluid injection rates (Kiel 1977; Zang et al. 2013). In “conventional hydraulic fracturing” relatively short-term monotonic fluid injection at relatively high injection rates is performed, resulting in relatively fast pressure build-up to levels above the fracturing pressure. Fatigue hydraulic fracturing mainly differs from conventional hydraulic fracturing in that fluid is injected in cycles with alternating higher and lower injection rates at different cycle times, resulting in a cyclic pressure response that gradually reaches the fracturing pressure over successive injection cycles (Hofmann et al. 2018). Fatigue hydraulic fracturing has been applied in laboratory experiments (Stephansson et al. 2019) as well as in a few field cases (Zang et al. 2019; Huenges et al. 2020). In some studies a decrease in formation breakdown pressure and increase of fracture disturbed zone has been found (Kiel 1977; Zang et al. 2019). These aspects are beneficial to reservoir stimulation as the likelihood of inducing seismicity may decrease due to lower injection pressures and volumes, while reservoir permeability and associated reservoir-to-well connectivity may increase due to the larger stimulated reservoir volume. An interesting aspect, compared with conventional hydraulic fracturing, is that the characteristics of injection cycles, such as duration, injection rate, frequency and number of stages, may be varied, yielding more operational parameters that can be optimized or tuned to different types of reservoirs. The effects on breakdown pressure and fracture network complexity may be attributed to progressive and enhanced microfracture development during stimulation and subcritical crack growth (Hofmann et al. 2018).

Subcritical crack growth has been observed in many in rock materials (Anderson and Grew, 1977; Atkinson 1982; Holder et al. 2001; Ko and Kemeny 2011), and is typically attributed to stress corrosion by chemical interactions at the crack tip at temperatures relevant to geothermal reservoirs (Atkinson 1982). Subcritical crack growth can lead to fracture propagation at stresses below the tensile or shear strength of rocks as described by conventional failure criteria, such as the Griffith and Mohr-Coulomb failure criteria (Figure 1). One of the main effects on rock fracturing is that it yields time dependence of fracture development and of decay of rock strength (Zhurkov 1984). Bungler and Lu (2015) modelled initiation of multiple fractures during (multistage) hydraulic fracturing in shales and found that subcritical crack growth controls stress-versus-strength conditions of fracture initiation.

Within the framework of soft stimulation and the overarching goal of the DESTRESS project, the relevance of subcritical crack growth to fatigue hydraulic fracturing is threefold:

- (1) Reduced injection rates and volumes are required for reservoir stimulation if subcritical crack growth leads to lower breakdown pressure, larger complexity of fracture networks and larger stimulated reservoir volume, which could lower the likelihood of induced seismicity,
- (2) Understanding the contribution of subcritical crack growth to fatigue hydraulic fracturing may lead to a mechanistic description of the process, which can be used to better predict and optimize the stimulation treatment,
- (3) Subcritical fracture propagation has the potential to progressively increase permeability and, hence, flow rates during operation of geothermal doublets without performing conventional hydraulic fracturing, provided reservoir conditions are such that the process is efficient and not counteracted by permeability-reducing processes such as fracture closure or scaling.

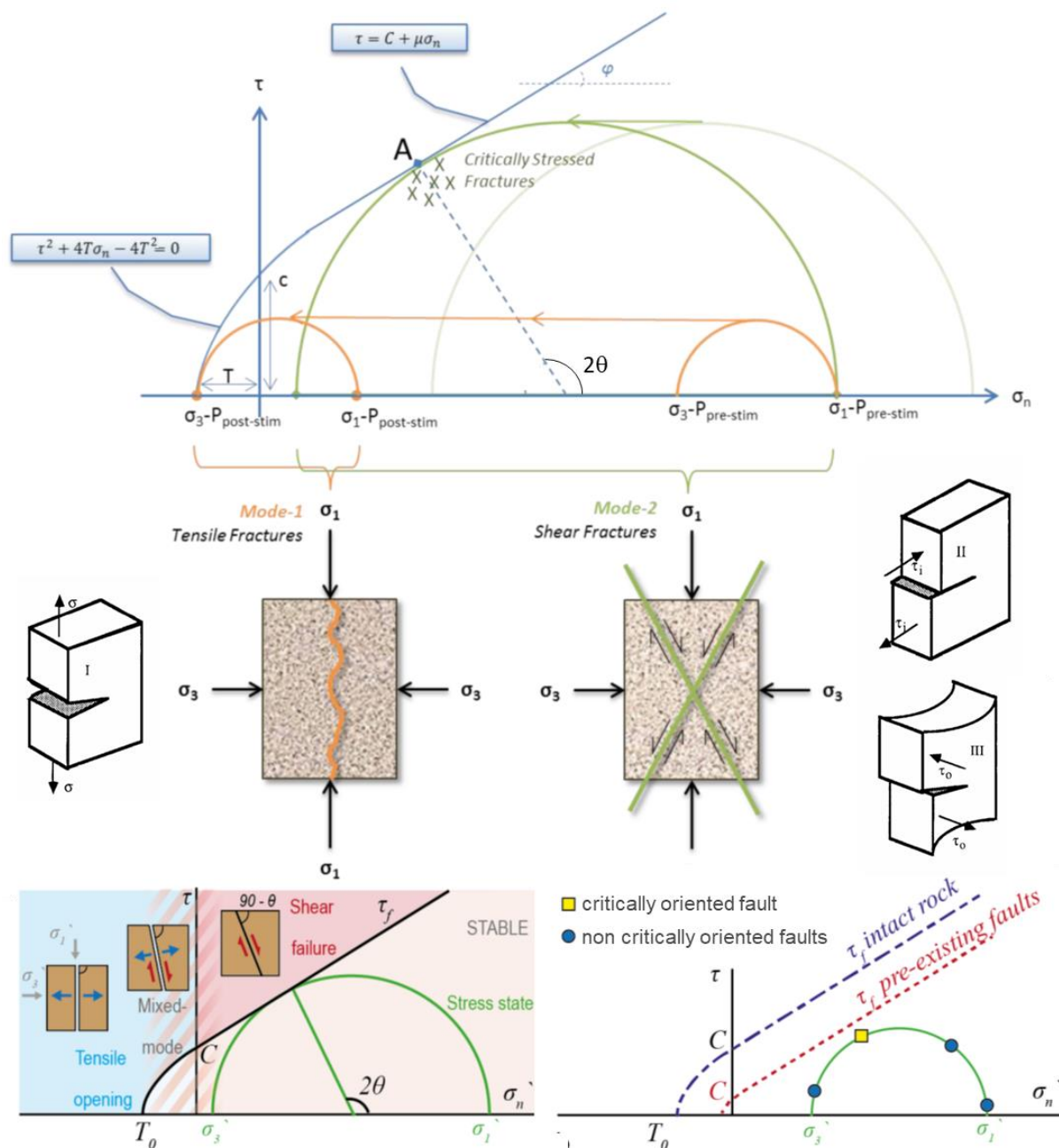


Figure 1 Schematic overview of geomechanical concepts relevant to fracturing of rocks. Top: Mohr-Coulomb Circle representation of the effect of increasing pore pressure on stress state and initiation of modes I and II fractures. For low differential stress ($\sigma_1 - \sigma_3$), increasing pore pressure leads to initiation of tensile (mode I) fractures (orange). For high differential stress, increasing pore pressure leads to initiation or reactivation of shear (mode II) fractures (green). Middle: Different fracturing modes I, II and III with schematic representation in rocks. Note that mode III is not indicated in the Mohr-Coulomb diagrams. Bottom: Link between fracture mode/orientation (θ) and stress state represented in a Mohr-Coulomb diagram (left). Difference in failure criterion of intact rock (fracture initiation criterion) and rock with pre-existing faults (fracture reactivation/hydraulic shearing criterion). Modified from: Veldkamp et al. (2015) and Buijze et al. (2019).

This study aims to explore methods to determine the contribution of subcritical crack growth in permeability increase during operation of a geothermal doublet targeting a tight sandstone reservoir in the Netherlands. It includes (1) a short review of the theory underpinning subcritical crack growth, (2) an analysis of typical experimental data for subcritical fracture growth velocities in sandstones, and

(3) an analysis of hydro-mechanical properties of the tight Triassic sandstone targeted by the Trias Westland project in the Netherlands.

2. Review of subcritical crack growth theory

Time-dependent subcritical fracture propagation and strength reduction have been observed under different loading conditions, i.e., for tensile (mode I) as well as shear (mode II) fractures (Ko and Kemeny 2008). The focus of the present study is on the role of mode I fracturing in reservoir stimulation by fluid injection. For a 2D mode I fracture opened at a constant pressure, the stress intensity factor (K_I) describes the resistance of a material to fracture propagation (Irwin 1957; Economides et al. 2000)

$$K_I = (P_f - \sigma_3)\sqrt{\pi L} \quad (1)$$

where P_f is the pressure in the fracture, σ_3 is the minimum principal stress and L is the fracture half-length. Fracture propagation velocity shows a complex relation with K_I , as a result of different mechanisms controlling the propagation velocity (Figure 2).

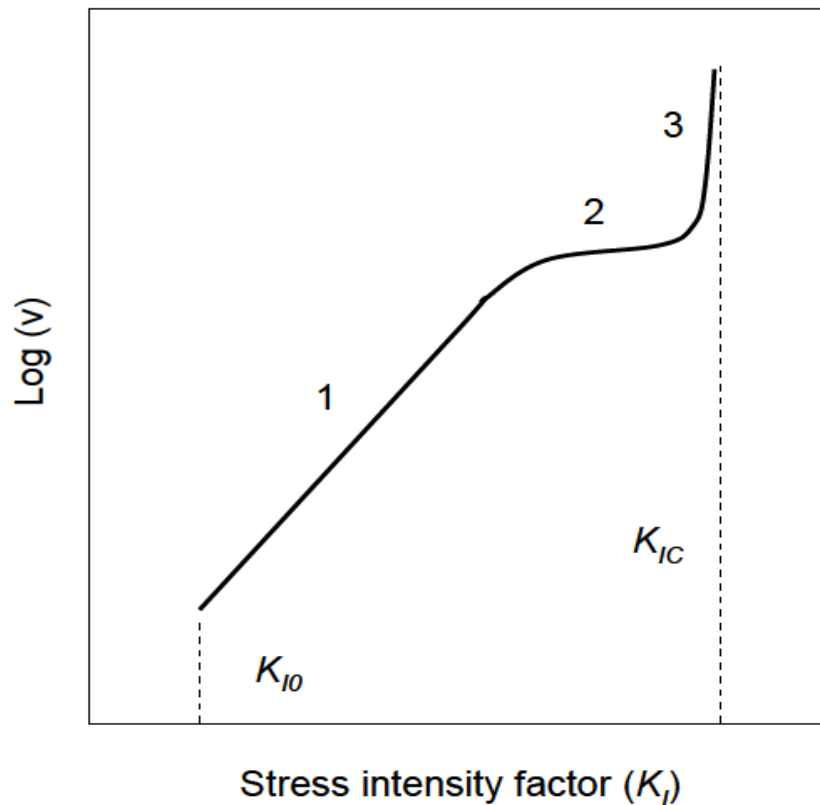


Figure 2 Relation between fracture propagation velocity (v) and stress intensity factors showing three regimes with different mechanisms that control propagation velocity.

Most experimental evidence suggest that subcritical crack growth occurs between a lower threshold value (K_{I0}) and the critical stress intensity fracture or fracture toughness (K_{IC}), although it is unclear if K_{I0} exists for all materials (Anderson and Grew 1977; Atkinson 1982). Atkinson (1982) suggested that in regime 1 fracture propagation velocity is controlled by stress corrosion reactions, transport of reactive species controls the velocity in regime 2, and velocity-controlling mechanisms in regime 3 are not fully understood. The most practical approach to describing the v - K_I relations in rocks is by a power law relation (Charles 1958; Atkinson 1982)

$$v = v_0 \exp(-\Delta H/RT) K_I^n \quad (2)$$

with v_0 a pre-exponential constant, ΔH an activation enthalpy, R the gas constant, T temperature and n the stress corrosion or subcritical crack growth index. If temperature is assumed constant and if K_I is expressed relative to material property K_{IC} , equation (2) yields

$$v = AK_I^n = A(K_I/K_{IC})^n \quad (3)$$

with pre-exponential constant A in [m/s]. Subcritical crack growth will lead to a time-dependent reduction in failure strength which can be expressed as time to failure (t) (Scholz 1972; Anderson and Grew 1977; Zhurkov 1984)

$$t = t_0 \exp \left[\frac{U_0 - \gamma \sigma_t}{RT} \right] \quad (4)$$

with t_0 , U_0 , γ material constants related to the oscillation frequency, binding energy, and disorientation of structure of atoms, and σ_t the tensile stress. For constant temperature, equation (4) can be simplified to

$$t = A \exp(-\alpha \sigma_t) \quad (5)$$

with pre-exponential constant A in [s] and constant α in [Pa^{-1}].

Most experimental data on subcritical crack growth in rock materials can be conveniently described by the above equations (Atkinson 1984). Data on subcritical crack growth velocities for mode I fractures can be used in numerical models to assess the contribution of subcritical fracture growth to stimulation of permeability in reservoirs (Lu et al. 2017). Subcritical crack growth may also contribute to reduction in shear failure strength (Ko and Kemeny 2011), which could lead to enhanced permeability by hydraulic shearing in fractured reservoirs.

3. Experimental data on subcritical crack growth in sandstones

Three experimental studies that have investigated fracture toughness and subcritical crack growth in sandstone were reviewed within the framework of this study (Senseny and Pfiefler 1984; Holder et al. 2001; Koh and Kemeny 2008). The experimental data are summarized in Table 1. Senseny and Pfiefler (1984) determined fracture toughness on sandstone samples collected at different depths (1311-2472 m) in the MWX wells drilled in the Piceance Basin. Short rod specimens with a chevron notch were used, following a method first proposed by Barker (1977). They found relatively large variations in fracture toughness (up to a factor of 3) between adjacent stratigraphic layers. Holder et al. (2001) determined subcritical crack growth velocities in weak, porous Scioto sandstone using a modified dual torsion beam test that includes a pre-loading procedure to minimize transient non-elastic material behaviour. Subcritical crack growth velocities between 10^{-6} and 10^{-2} m s⁻¹ were measured for stress intensity factors between 0.5 and 0.7 MPa m^{1/2}. Besides some typical values for the subcritical crack growth index and the pre-exponential constant that can be used in equation (3) to describe subcritical crack growth velocity, they found lower n values under water-saturated conditions compared to samples exposed to air. Koh and Kemeny (2008) determined both fracture toughness and subcritical crack growth parameters in Coconino sandstone by varying loading rates on Brazilian and grooved disk specimens for mode I parameters, on rectangular single shear specimens for mode II parameters, and rectangular punch-through specimens for mode III parameters. A reduction in tensile strength of ~17% was found if loading rate were decreased from 10 MPa/s to 0.01 MPa/s.

Study		K_{IC} [MPa.m ^{1/2}]	n	A [m.s ⁻¹]
Senseny & Pfiefler (1984)		0.69-2.40 (1.27)	-	-
MWX wells, Piceance Basin				
Holder et al. (2001)	air	-	35 ± 5 (38.5)	1.29x10 ⁻⁵
Scioto sandstone			52	
E = 11.4 GPa	water	-	25	
ν = 0.13			36	
Koh & Kemeny (2008)				
Coconino sandstone	mode I	0.66-0.78 (0.72)	37 ± 11	4.2x10 ⁻² ± 1.7x10 ⁻³
UCS: 118 ± 3 MPa	mode II	1.12-1.37 (1.27)	35 ± 13	2.2x10 ⁻² ± 9.9x10 ⁻⁴
σ_t = 6.4 ± 0.9 MPa	mode III	-	37 ± 9	-
E = 24.3 ± 1.5 GPa				
ν = 0.36 ± 0.03				
C_0 = 22.7 MPa				
ϕ = 50.6°				

Table 1 Summary of experimental data on subcritical crack growth in sandstones from three studies. Fracture toughness (K_{IC}), subcritical crack growth index (n) and pre-exponential constant A

4. Geomechanical characteristics of the Triassic sandstone targeted by the Trias Westland project

The Trias Westland geothermal project in the Netherlands drilled to a Triassic sandstone reservoir at ~4.3 km depth. Well tests and core analysis indicate that the reservoir was too tight to be successfully developed. Core analysis showed helium porosity values of 1.4-3.9% and Klinkenberg permeability below 0.02 mD (Felder and Fernandez 2018). Currently, geothermal operations continue in shallower (~2.3 km) Lower Cretaceous sandstones. Given the cost of drilling to ~4.3 km, it is of interest to explore possibilities to stimulate reservoir permeability. Core material from the NLW-GT-01 Trias Westland well was made available for the current DESTRESS study, providing unique access to reservoir rock samples from a deep geothermal well. The full core was sampled and made available for research, allowing core samples perpendicular (roughly horizontal plugs) and parallel (roughly vertical plugs) to the axis of the core to be drilled.

The current experiments focus on determining hydro-mechanical properties of the tight sandstone reservoir rock. Considering the importance for flow properties as well as for triaxial axial compression experiments, a lot of effort was put in obtaining information on saturation and poroelastic properties of the sandstone and on building a setup that allows hydraulic and subcritical fracturing to be studied in a triaxial deformation apparatus. Three triaxial experiments and three fluid injection experiments were performed on the core samples (~50 mm length and ~25 mm diameter) of the NLW-GT-01 well at different confining and injection pressures (Table 2). Two samples (NLW-GT-01-14H, and NLW-GT-01-15H) were drilled perpendicular to the axis of the core, and four (NLW-GT-01-4V, NLW-GT-01-6V, NLW-GT-01-7V, and NLW-GT-01-8V) were drilled parallel to the core axis. Duration and pressure history of the triaxial experiments varied between relatively short term (5.5 hr) experiments with a monotonic pressure increase and axial loading, and relatively long term (146.6 and 246.1 hr) experiments with more complex pressure history, followed by monotonic axial loading. Confining pressures ($P_c = S_3$) ranged between 5 and 53 MPa; all experiments were performed at room temperature.

The relatively short term triaxial experiment was performed at $P_c = 53.0$ MPa, roughly representative of the minimum horizontal stress ($S_{hmin} = S_3$) at 4 km depth in the prevailing normal faulting regime in the Netherlands (i.e. assuming $\Delta S_v/\Delta Z = 22$ MPa/km, $S_{hmin}/S_v = 0.6$ and $S_{hmin} = S_{Hmax}$). Upstream and downstream pressures (P_u and P_d) were vented to atmosphere to ensure drained conditions, which can be compared with the relatively long term experiments at elevated P_u and P_d .

For the relatively long term triaxial experiments, upstream and downstream pressures (P_u and P_d) were varied between 0.0 and 46.0 MPa, with $P_u = P_c$ to test saturation, pore connectivity and poroelastic properties and $P_u > P_c$ to perform (Darcy) flow tests. Long term (143.3 and 237.2 hr) saturation, pressurization, flow and poroelastic stressing stages were performed prior to deformation in axial compression. Initial saturation stages of 65.0-70.4 hr duration were performed at lower P_c of 0.5 and 15.0 MPa. The flow test was performed on sample NLW-GT-01-14H by applying $P_u = 10$ MPa and P_c vented to atmosphere for 22.5 hr. In the poroelastic stressing stages, P_c was increased by (typically) 1 MPa at 1 MPa/hr, followed by 30-90 minutes pressure equilibration for each step, while P_u and P_c were continuously monitored. It should be emphasized that although the poroelastic stressing stages were performed following the approach originally proposed by Skempton (1954), the lack of permeability and associated lack of pore connectivity hamper reliable assessment of Skempton B-coefficients and saturation. It has been suggested that pore pressure changes caused by changes in P_c become constant at increasing confinement, indicating full saturation of rock samples (Makhnenko and Labuz 2013). However, results of the current poroelastic stressing stages do not indicate such a trend, and suggest that the combined compressibility of bulk sample and fluid system to upstream and

downstream pressure sensors is recorded rather than separate contributions of pore fluid and the rock framework (Fjaer et al. 2008).

Sample	Test stage	Duration [hr]	σ_1 [MPa]	$\sigma_2 = \sigma_3$ [MPa]	Upstream Pressure [MPa]	Downstream Pressure [MPa]
NLW-GT-01-14H (4263 m MD)	1. ambient saturation	70.4	0.5	0.5	vent	vent
	2. pressurizing	0.2	15.0	15.0	vent	vent
	3. Darcy flow	22.5	15.0	15.0	10	vent
	4. pressurizing	19.6	25.0	25.0	17.3-25.0	17.3-25.0
	5. poroelastic stressing	4.1	25-30	25-30	closed	closed
	6. axial compression	1.6	max. 168.8	30.0	27.8	closed
	7. de-pressurizing	1.6	unload	0	vent	vent
NLW-GT-01-15H (4264 m MD)	1. saturation	65.0	15.0	15.0	vent	vent
	2. pressurizing	24.0	16.0	16.0	0.0-2.0	0.0-2.0
	3. poroelastic stressing	6.6	16-20	16-20	closed	closed
	4. pressurizing	17.4	20.0	20.0	max. 13.0	max. 13.0
	5. poroelastic stressing	7.2	20-27	20-27	closed	closed
	6. pressurizing	16.6	27.0	27.0	max. 18.3	max. 23.4
	7. poroelastic stressing	25.7	27-53	27-53	closed	closed
	8. pressurizing	74.6	53.0	53.0	46.0	46.0
	9. axial compression	1.3	max. 214.9	53.0	46.4	46.4
	10. de-pressurizing	2.2	unload	0	vent	vent
NLW-GT-01-7V (4256.06 m MD)	1. pressurizing	2.9	53.0	53.0	0.1	vent
	2. axial compression	2.6	max. 394.6	53.0	0.1	vent
NLW-GT-01-4V (4253.1 m MD)	1. pressurizing	1.6	44.0	32.0	20.0	20.0
	2. fluid injection, P_{max}^*	1.8	45.4	32.1	45.7	15.0
NLW-GT-01-6V (4255.06 m MD)	1. pressurizing	1.2	8.8	5.0	5.0	5.0
	2. fluid injection, P_{max}^*	1.2	12.7	5.0	22.8	5.0
NLW-GT-01-8V (4257.05 m MD)	1. pressurizing	1.4	15.0	5.0	0.5	0.5
	2. fluid injection, P_{max}^*	0.6	14.8	5.0	20.3	0.5

Table 2 Summary of test stages for experiments on core samples from the NLW-GT-01 well drilled for the Trias Westland geothermal project. Conditions reached after each stage are quoted. MD denotes measured depth along the well. * P_{max} -conditions at maximum injection pressure before (jacket) failure (connected to upstream fluid inlet, see text).

After saturation and pressurization stages at isotropic stress state, three samples (NLW-GT-01-14H, NLW-GT-01-15H and NLW-GT-01-7V) were deformed in axial compression to determine Young's modulus as well as failure and residual strength. Axial compression of samples was achieved using a lower ram to move the triaxial cell with lower and upper pistons (25 mm diameter), sample and internal load cell against an external load cell mounted on the crosshead of the loading frame. The samples were sealed with respect to the oil confining medium using a jacket made heat shrinking tube. A constant displacement rate of the lower ram yielded axial strain rates of $\sim 5 \times 10^{-6} \text{ s}^{-1}$. The triaxial cell allows for independent control of axial and radial stresses (confinement) as well as upstream and downstream pressures. Axial stress was measured by two load cells, located both inside and outside the pressure vessel. Confining pressure and upstream and downstream pressures were controlled via external pumps. Axial strains were measured indirectly by means of an external linear variable differential transformer (LVDT) only, implying that the combined displacement due to both sample deformation and load-dependent elastic shortening of the piston assembly is recorded. Therefore,

axial strains measured by this setup are likely overestimated, possibly leading to underestimation of sample stiffness (Young's modulus). Radial strains were not measured. Fluid injection experiments were performed in a similar setup to that used for the axial compression tests. Differences are that the upper and lower pistons are oversized (35 mm diameter) with respect to the ~25 mm diameter sample to accommodate sealing O-rings around the sample at the piston-sample interface, and that the upstream pressure was connected through the upper piston and a metal spacer to a ~4 mm hole drilled in the centre of the sample. The metal spacer ($L \times D = 25 \times 25$ mm) had circular grooves on both end with ~10 cm diameter O-rings to prevent pressure communication between injected fluid and the outside of the sample and spacer. A ~3.7 mm diameter hollow metal pressure tube was glued into the central hole in the sample using epoxy resin and sealed at the top by a ~4 mm O-ring to ensure that fluid was injected roughly at the centre of the sample.

Results of the saturation and poroelastic stressing tests confirmed the low permeability found in the well tests and previous core analysis: i.e. (1) poroelastic stressing does not indicate effects of increasing saturation; and (2) the Darcy flow test does not indicate any flow across the sample. The axial compression tests indicated a Young's modulus (E) of 12.9-17.6 GPa and a high failure strength of 394.6 MPa at $P_c = 53.0$ MPa if $P_u = 0.1$ MPa and P_c is vented to atmosphere (sample NLW-GT-01-7V, Figure 3).

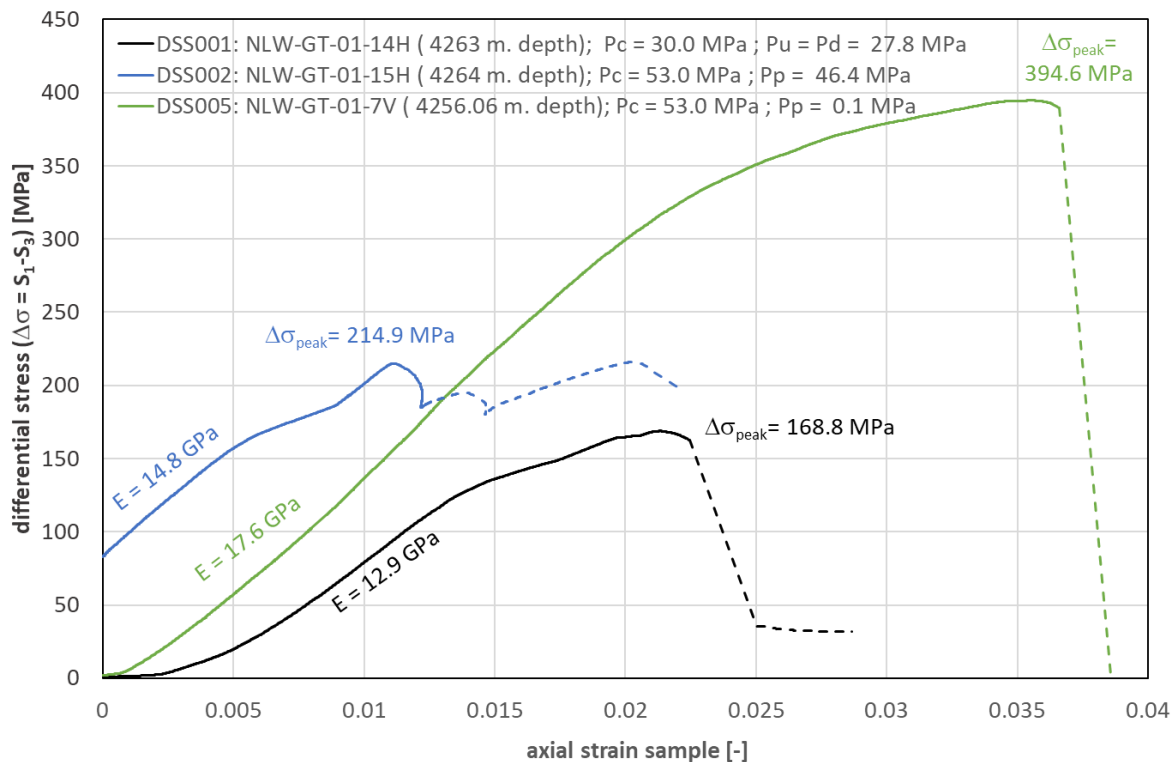


Figure 3 Stress-strain curves for triaxial experiments on samples NLW-GT-01-14 and NLW-GT-01-15, deformed in axial compression. Dashed parts of curves indicate post failure behaviour with axial strains that are affected by elastic response of the deformation apparatus due to unloading of the piston-sample assembly (note that axial displacement is measured externally, see text).

Failure strengths of 168.8 MPa and 214.9 MPa were found at elevated P_u and P_d and $P_c = 30.0$ MPa and $P_c = 53.0$ MPa (samples NLW-GT-01-14H and NLW-GT-01-15H, respectively). Post failure behaviour is markedly different for the three samples. NLW-GT-01-14H and NLW-GT-01-15H show a relatively sharp decrease in stress after the peak stress down to a residual stress or to zero strength, respectively. In

contrast, post failure stresses in NLW-GT-01-15 show multiple peaks after failure. This difference might have a range of causes, but is most likely due to the difference in confining and pore pressures.

The results of the fluid injection tests are more difficult to interpret as all tests indicate a failure of the sample jacket and pressure communication between P_c , P_u and P_d at injection pressures of $P_i = 20.3$ - 45.7 MPa. It is uncertain if tensile fracturing of the sample caused jacket failure, or if jacket failure resulted from failure of O-ring seals. In any case, the pressure difference $\Delta P_i = P_i - P_c$ (13.6-17.7 MPa) can be regarded as a lower bound to the injection pressure in the central hole that is required for tensile fracturing to occur.

The failure strengths can be plotted on a Mohr-Coulomb failure diagram (Figure 4). Although based on only three triaxial failure tests, a linear Mohr Coulomb failure criterion with friction coefficient ($\mu_u = 0.7$) and cohesion ($S_0 = 50$ MPa) can be used to cap all stress states at failure (indicated by Mohr circles). An unconfined compressive strength (UCS) of 198.0 MPa can be estimated based on these values (Al-Ajmia and Zimmerman 2005). The experiment on sample NLW-GT-01-14H seems to indicate that a lower differential stress is required to reach failure, which could be caused by the different duration or pressure history. Additional triaxial experiments should be performed to confirm or reject this suggestion. If a systematic relation between duration and pressure history and failure strength is confirmed by additional tests, it could be indicative of an effect of subcritical crack growth on failure strength. An alternative explanation is sample variability. The mechanical properties are consistent with a relatively strong, low porosity and permeability sandstone (Fjaer et al. 2008).

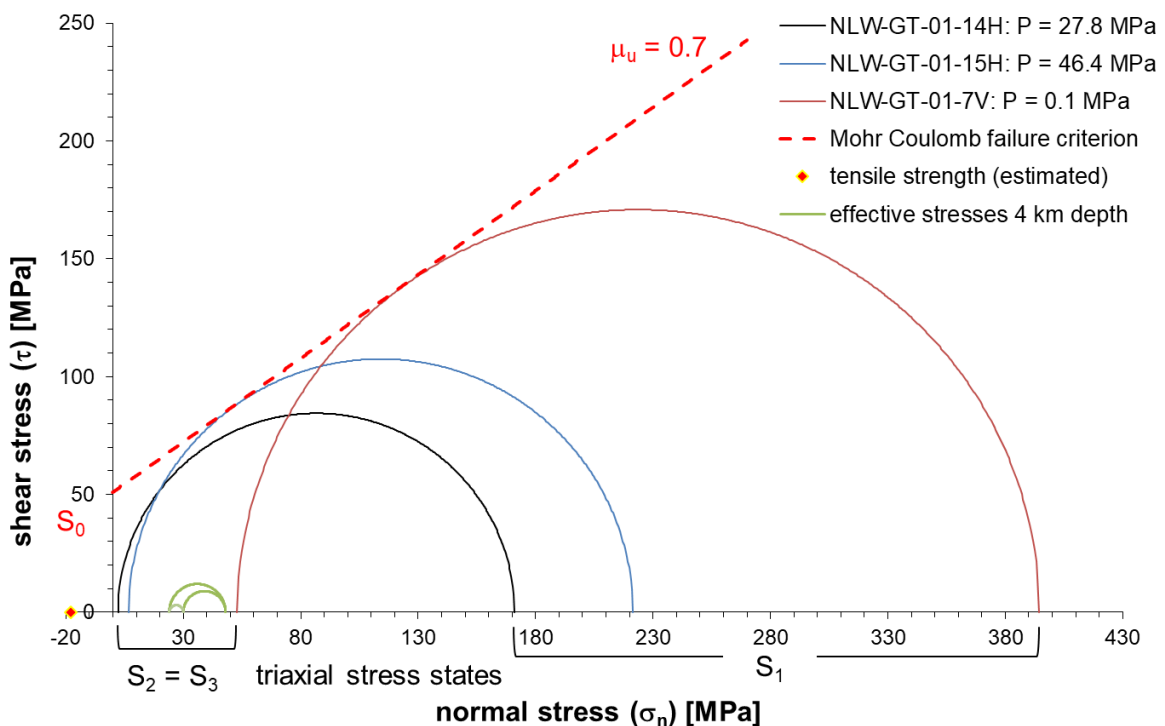


Figure 4 Mohr circle diagrams representing the stress state at failure for samples NLW-GT-01-14 and NLW-GT-01-15, deformed in axial compression. Two (end member) cases are shown, assuming full or no saturation of pores. A typical stress state at ~4 km depth in the Netherlands is indicated for reference (normal faulting regime with $S_1=S_v$, $S_2=S_{Hmax}$, $S_3=S_{Hmin}$ and $\Delta S_v/\Delta Z = 22$ MPa, $\Delta S_{Hmin}/\Delta Z = 16$ MPa, $S_{Hmin}/S_{Hmax} = 0.9$). See text for further details and meaning of symbols.

5. Discussion

Fatigue hydraulic fracturing involving cyclic increase and decrease of fluid injection rates has been suggested to lead to lower formation breakdown pressure and enlargement of the fracture disturbed zone (Kiel 1977; Zang et al. 2013). It may be beneficial to reservoir stimulation as the likelihood of inducing seismicity may decrease, while reservoir permeability and associated reservoir-to-well connectivity may increase. Subcritical crack growth may be one of the controlling microphysical processes that, if properly understood and quantified, can contribute to more efficient, low risk stimulation of reservoir permeability by (1) reduction of injection rates and volumes required for stimulation, (2) better optimization of stimulation, and (3) progressively increasing permeability and flow rates during operation of geothermal doublets. This review of subcritical crack growth theory and experiments on tight sandstones suggest that this process can contribute to permeability increase during operation of geothermal doublets, but its efficiency for enhancing permeability of geothermal reservoirs remains unclear.

This study provides the first data on both tensile and shear failure of the tight Triassic sandstone targeted by the Trias Westland project in the Netherlands. The hydro-mechanical properties of the sandstone, as determined in laboratory experiments, suggest that this reservoir is too tight to be considered for geothermal energy. Flow rates will be negligible unless the low reservoir permeability is restricted to the near-well area or high permeability zones exist that can be connected to wells using stimulation treatments. Disentangling the effect of subcritical crack growth in conventional triaxial experiments on rock materials is not straightforward. It requires detailed characterization of the hydro-mechanical behaviour of the rock materials to identify deviations from conventional behaviour that can be explained by subcritical crack growth. As subcritical crack growth theory depicts fracturing behaviour that is dependent on time and pressure history, long term tests are required to demonstrate effects of subcritical crack growth. Core samples of the reservoir rocks provide an excellent opportunity to further study the effect of stimulation, including the effect of subcritical crack growth on permeability and strength.

6. Conclusions

The following main conclusions are made by the current study:

1. The review of subcritical crack growth theory and experiments on tight sandstones suggest that this process can contribute to permeability increase during operation of geothermal doublets, but its efficiency in enhancing permeability of geothermal reservoirs remains unclear.
2. The Triassic sandstone reservoir targeted by well NLW-GT-01 is relatively stiff and strong sandstone with very low permeability as indicated by its moderate Young's modulus ($E = 12.9\text{-}17.6$ GPa), high cohesion ($S_0 = 50$ MPa), estimated unconfined compressive strength ($UCS = 198$ MPa), and estimated lower bound to tensile strength (13.6-17.7 MPa).
3. The NLW-GT-01 dataset provides a first indication of the hydro-mechanical properties and failure behaviour of this sandstone. Further experiments should be performed to identify time- and pressure history dependence of failure strengths, and to demonstrate the effect of subcritical crack growth on permeability and strength.
4. Subcritical crack growth may contribute to more efficient, low risk stimulation of reservoir permeability by (1) reduction of injection rates and volumes required for stimulation, (2) better optimization of stimulation, and (3) progressively increasing permeability and flow rates during operation of geothermal doublets.

7. References

- Anderson, O. L., and Grew, P. C. (1977), Stress corrosion theory of crack propagation with applications to geophysics, *Rev. Geophys.*, 15(1), 77– 104, doi:[10.1029/RG015i001p00077](https://doi.org/10.1029/RG015i001p00077).
- Atkinson, B.K. (1982). Subcritical crack propagation in rocks: theory, experimental results and applications, *Journal of Structural Geology*, 4, 41-56, [https://doi.org/10.1016/0191-8141\(82\)90005-0](https://doi.org/10.1016/0191-8141(82)90005-0).
- Bunger, A. P., Lu, G. (2015). Time-dependent initiation of multiple hydraulic fractures in a formation with varying stresses and strength. Society of Petroleum Engineers. doi:10.2118/171030-PA.
- Buijze, L., Van Bijsterveldt, L., Cremer, H., Paap, B., Veldkamp, H., Wassing, B., Van Wees, J.-D, Ter Heege, J. Review of worldwide geothermal projects: mechanisms and occurrence of induced seismicity. TNO report | TNO 2019 R100043. www.nlog.nl/scan
- Charles, R. J. (1958). Dynamic fatigue of glass. *J. appl. Phys.* 29, 1657-1662.
- Economides, M.J., Nolte, K.G. (2000). Reservoir stimulation, 3rd edition. Chichester, UK. John Wiley & Sons.
- Felder, M., Fernandez, S. (2018). Core Hot Shot NLW-GT-01. Panterra Geoconsultants, report G1340_3/c18008, www.nlog.nl.
- Fjaer, E., Holt, R.M., Horsrud, A.M.R.P. (2008). Petroleum Related Rock Mechanics, Volume 53, 2nd Edition.
- Hofmann, H., Zimmermann, G., Zang, A. *et al.* (2018). Cyclic soft stimulation (CSS): a new fluid injection protocol and traffic light system to mitigate seismic risks of hydraulic stimulation treatments. *Geotherm Energy* 6, 27. <https://doi.org/10.1186/s40517-018-0114-3>.
- Holder, J., Olson, J.E., Philip, Z. (2001). Experimental determination of subcritical crack growth parameters in sedimentary rock. *Geophys. Res. Lett.* 28, 4, <https://doi.org/10.1029/2000GL011918>.
- Huenges, E., Ellis, J., Welter, S., Westaway, R., Min, K.B., Genter, A., Brehme, M., Hofmann, H., Meier, P., Wassing, B., Marti, M. (2020). Demonstration of soft stimulation treatments in geothermal reservoirs. Proceedings World Geothermal Congress 2020, Reykjavik, Iceland, April 26 – May 2, 2020.
- Irwin, G. R. (1958). Fracture. In: *Handbuch der Physik* 6 (edited by Flugge, S.). Springer, Berlin, 551-590.
- Kiel, O. M. (1977). The Kiel process reservoir stimulation by dendritic fracturing. Society of Petroleum Engineers.
- Ko, T. Y., & Kemeny, J. (2008). Experimental study of subcritical crack growth under mode I, mode II and mode III loading. American Rock Mechanics Association.
- Ko, T. Y., and Kemeny, J. (2011), Subcritical crack growth in rocks under shear loading, *J. Geophys. Res.*, 116, B01407, doi:[10.1029/2010JB000846](https://doi.org/10.1029/2010JB000846).

- Ko, T.Y., Kemeny, J. (2013). Determination of the subcritical crack growth parameters in rocks using the constant stress-rate test, *International Journal of Rock Mechanics and Mining Sciences*, 59, 166-178, <https://doi.org/10.1016/j.ijrmms.2012.11.006>.
- Lu, G. Gordeliy, E., Prioul, R., Bungler, A. (2017). Modeling initiation and propagation of a hydraulic fracture under subcritical conditions, *Computer Methods in Applied Mechanics and Engineering*, 318, 61-91, <https://doi.org/10.1016/j.cma.2017.01.018>.
- Makhnenko, R. Y., & Labuz, J. F. (2013). Saturation of Porous Rock and Measurement of the *B* Coefficient. American Rock Mechanics Association.
- Scholz, C. H. (1972). Static fatigue of quartz. 3. *J. Geophys. Res.* 77, 2104-2114.
- Senseny, P. E., & Pfeifle, T. W. (1984). Fracture Toughness Of Sandstones And Shales. American Rock Mechanics Association.
- Skempton, A.W. (1954). The pore-pressure coefficients *A* and *B*. *Geotechnique*, 4, 143-147.
- Stephansson, O., Semikova, H., Zimmermann, G. *et al.* (2019). Laboratory Pulse Test of Hydraulic Fracturing on Granitic Sample Cores from Äspö HRL, Sweden. *Rock Mech Rock Eng* **52**, 629–633. <https://doi.org/10.1007/s00603-018-1421-5>.
- Zang, A. Yoon, J.S., Stephansson, O., Heidbach, O. (2013). Fatigue hydraulic fracturing by cyclic reservoir treatment enhances permeability and reduces induced seismicity, *Geophysical Journal International*, 195, 1282–1287, <https://doi.org/10.1093/gji/ggt301>.
- Zang, A., Zimmermann, G., Hofmann, H. *et al.* (2019). How to Reduce Fluid-Injection-Induced Seismicity. *Rock Mech Rock Eng* **52**, 475–493 <https://doi.org/10.1007/s00603-018-1467-4>.
- Zhurkov, S.N. (1984). Kinetic concept of the strength of solids. *Int J Fract* **26**, 295–307. <https://doi.org/10.1007/BF00962961>.

Imprint

Project Lead	GFZ German Research Centre for Geosciences Telegrafenberg 14473 Potsdam (Germany) www.gfz-potsdam.de/en/home/
Project Coordinator	Prof. Ernst Huenges huenges@gfz-potsdam.de +49 (0)331/288-1440
Project Manager	Dr. Justyna Ellis ellis@gfz-potsdam.de +49 (0)331/288-1526
Project Website	www.destress-h2020.eu
Copyright	Copyright © 2020, DESTRESS consortium, all rights reserved

Liability claim

The European Union and its Innovation and Networks Executive Agency (INEA) are not responsible for any use that may be made of the information any communication activity contains.

The content of this publication does not reflect the official opinion of the European Union. Responsibility for the information and views expressed in the therein lies entirely with the author(s).

DESTRESS is co-funded by

National Research Foundation of Korea (NRF)
Korea Institute for Advancement of Technology (KIAT)
Swiss State Secretariat for Education, Research and Innovation (SERI)